Boat extraction in harbors from high resolution satellite images using mathematical morphology and marked point processes

Paula Craciun, Josiane Zerubia

Boat extraction in harbors from high resolution satellite images using mathematical morphology and marked point processes

Paula Crăciun, Josiane Zerubia*

AYIN research group INRIA Sophia-Antipolis Méditerranée
2004 Route des Lucioles, BP 93, 06902 Sophia-Antipolis Cedex (France)
Firstname.Lastname@inria.fr

Résumé – L'extraction de bateaux dans des ports à partir d'images de télédétection haute résolution est une tâche très difficile, en raison de la répartition particulière des bateaux. Un modèle de processus ponctuel marqué a été mis au point pour résoudre ce problème. Ce modèle utilise une série de paramètres, dont certains sont déterminés à la main par essais et erreurs. Dans cet article, nous utilisons la morphologie mathématique pour détecter automatiquement l'orientation globale des objets d'intérêt, qui est un paramètre clé du modèle.

Abstract – Boat extraction in harbors from high resolution remotely sensed imagery is a very difficult task, due to the particular distribution of the boats. A marked point process model has been devised for solving this task. This model uses a series of parameters, some of which are determined by hand through trial and error techniques. In this paper, we use mathematical morphology to automatically determine the global orientation of the objects, which is a key parameter of the model.

1 Introduction

The problem of feature extraction from remotely sensed imagery has been widely addressed throughout literature, varying from pixel-based to object-based approaches and having a multitude of applications ranging from civilian to military ones. As the resolution of the aerial and recent satellite images is very high, pixel-based approaches have found their limits in object extraction. The main cause is the necessity to cope with situations where objects are unevenly illuminated, partially occluded or blended with the background.
Thus, in the case of high-resolution satellite imagery (i.e. GeoEye, Pleiades), object-based solutions are preferred. A framework for such solutions is provided by stochastic geometry. The quest is to look for a pattern that fits the objects in an image, considered to be a realization of a random process. Three ingredients are needed to build a spatial pattern analysis tool: the conditional probability depending on the data, the prior used to give a general aspect of the searched solution and an optimization method. In this regard, marked point processes (MPPs) were introduced by mathematicians to solve pattern analysis problems [3, 4]. Following this approach, solutions arising to problems from high-resolution remotely sensed imagery were brought by developing more complex models to deal with different types of objects [2, 7].
On the other hand, mathematical morphology, introduced by J. Serra, proved its usefulness in the field of image processing [8]. Ingenious operators and methods have been devised to identify and underline some morphological features in the image.
In this paper, we propose to use mathematical morphology as a preprocessing step for detecting global directional features in the image, features which allow us to increase the quality of the object extraction by means of the MPP framework. The paper is organized into two parts. The first part presents a theoretical study of the MPP model used for object extraction. The second part presents a mathematical morphology tool, called rose of directions, that is used to determine the global orientation of the objects to be extracted. Finally, we will show how these tools are merged to solve the problem of boat extraction in harbors.

2 Extraction of boats in harbors using MPPs

MPP models have received increased attention in spatial statistics and have been applied to image processing with success. In this paper we will consider a particular model that was developed in [1] to extract elliptical objects. The

*We thank the French Space Agency (CNES) for providing the data, Saima Ben Hadj from INRIA/I3S for fruitful discussions and Antoine Mangin from ACRI-ST for useful feedback regarding the model.

main advantage of this model relies on the existence of a physical interpretation of some of its associated parameters.
We consider a marked point process of ellipses. The object space $\mathcal{W}$, is a bounded set in $\mathbb{R}^5$:

$$\mathcal{W} = [0, X_M] \times [0, Y_M] \times [a_m, a_M] \times [b_m, b_M] \times [0, \pi]$$

where X_M and Y_M are the width and height of the input image, respectively, a_m and a_M are the minimum and the maximum of the semi-major axis of the ellipse, b_m and b_M are the minimum and the maximum of the semi-minor axis of the ellipse and $\omega \in [0, \pi]$ is the orientation of the ellipse. An ellipse is parameterised as shown in Figure 1 (left).

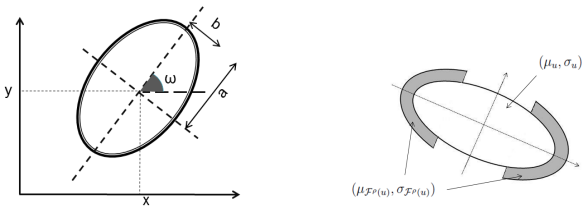

FIG. 1: left: Parameterization of an ellipse; right: Exterior border considered for the computation of the data energy term

We are interested in a particular class of MPPs, called Gibbs processes [10]. These processes enable us to model the different interactions between objects. The probability density function of such a process is given by:

$$f_\theta(X = \mathbf{x}|\mathbf{y}) = \frac{1}{c(\theta|\mathbf{y})} \exp^{-U_\theta(\mathbf{x},\mathbf{y})}$$

where $c(\theta|\mathbf{y})$ is a normalizing function with this form:

$$c(\theta|\mathbf{y}) = \int_\Omega \exp^{-U_\theta(\mathbf{x},\mathbf{y})\mu(d\mathbf{x})}.$$

θ is a parameter vector which allows the model to be flexible, in order to fit different images, $\mu(\cdot)$ is the intensity measure of the reference Poisson process, $U_\theta(\mathbf{x}, \mathbf{y})$ is called the energy, Ω is the configuration space, $\mathbf{x}$ denotes the object configuration and $\mathbf{y}$ denotes the image.
The energy function $U_\theta(\mathbf{x}, \mathbf{y})$ is divided into two types of energies. One is called data energy $U_\theta^d(\mathbf{x}, \mathbf{y})$, and it represents the configurations fidelity with respect to the input image. The second is called prior energy $U_\theta^p(\mathbf{x})$ and reflects knowledge about the objects to be extracted. If we use the MAP criterion then the most likely configuration which allows the extraction of objects corresponds to the global minimum of the total energy $U_\theta(\mathbf{x}, \mathbf{y})$:

$$x \in \underset{\mathbf{x}\in\Omega}{Argmax}\ f_\theta(X = \mathbf{x}|\mathbf{y}) = \underset{\mathbf{x}\in\Omega}{Argmin}[U_\theta(\mathbf{x}, \mathbf{y})].$$

Once the parameter vector θ is determined, a solution to this optimization problem can be found by means of simulated annealing combined with a sampling algorithm such as Reversible Jump MCMC [5]. Parameter estimation techniques are not presented here, for more details, see [1, 2].

2.1 The data energy term

The data energy term is modeled locally, for each object in the configuration. Thus, the total data energy of a configuration $\mathbf{x}$ is:

$$U_{\theta_d}^d(\mathbf{x}, \mathbf{y}) = \gamma_d \sum_{u\in\mathbf{x}} U_d(u),$$

γ_d being the weight of the data energy and θ_d is the parameter vector associated to it. The data energy relies on computing a distance measure between the distributions of the set of pixels belonging to the object u and the set of pixels belonging to its border $\mathcal{F}^\rho(u)$, as shown in Figure 1 (right).
The local data energy is built as a qualification of this contrast measure, thus favoring well positioned objects (i.e. high contrast between the interior and the border of the object) while penalizing misplaced ones:

$$U_\theta^d(u) = \mathcal{Q}(\frac{d(u, \mathcal{F}^\rho(u))}{d_0})$$

where $d(u, \mathcal{F}^\rho(u))$ is the modified Bhattacharya distance [10] between the object u and its boundary $\mathcal{F}^\rho(u)$ of width ρ and d_0 is a threshold for that distance. $\mathcal{Q} : \mathbb{R}^+ \rightarrowtail [-1, 1]$ is a quality function and attributes a negative value to well placed objects (e.g. those objects u for which $d(u, \mathcal{F}^\rho(u))$ is higher than the threshold d_0) and a positive value to misplaced objects. $\mathcal{Q}(x)$ is defined using a cubic root which allows a moderate penalization when the distance is close to the threshold:

$$\mathcal{Q}(x) = \begin{cases} 1 - x^{1/3} & \text{if } x < 1 \\ exp(-\frac{x-1}{3}) - 1 & \text{if } x \geq 1 \end{cases}$$

The quality function is plotted in Figure 2 (left).

2.2 The prior energy term

This energy term consists of two parts. One corresponds to a penalization of overlapping objects, avoiding the detection of the same object several times. The proposed model uses a *hard core* process to handle object overlapping. Thus, denoting by $A(x_i, x_j) = \frac{Area(x_i \cap x_j)}{\min(Area(x_i), Area(x_j))}$ the area of intersection between the objects x_i and x_j, the prior energy can be defined as:

$$U_o^p(\mathbf{x}) = \sum_{1<i\neq j<n(\mathbf{x})} t_s(x_i, x_j)$$

with:

$$t_s = \begin{cases} 0 & \text{if } A(x_i, x_j) < s \\ +\infty & \text{otherwise} \end{cases}$$

where $s \in [0, 1]$ corresponds to the amount of overlapping allowed by the model and $n(\mathbf{x})$ is the number of objects in the configuration $\mathbf{x}$. Accordingly, all configurations containing at least two objects that overlap to a higher ratio than specified by s are prohibited.

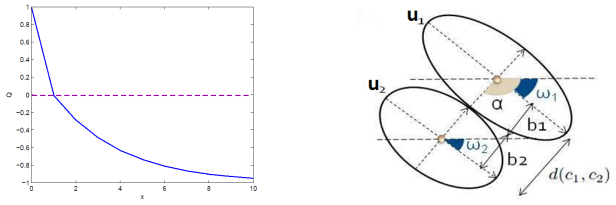

FIG. 2: left: Quality function; right: Alignment interaction between two elipses

The second part is used to favor close and aligned ellipses sharing the same global orientation. The alignment interaction $\sim_{al}$ between two ellipses e_1 and e_2 is defined as:

$$e_1 \sim_{al} e_2 \Leftrightarrow \begin{cases} d_\omega(e_1, e_2) \leq d_{\omega_{max}} \\ d_\alpha(e_1, e_2) \leq d_{\alpha_{max}} \\ d_C(e_1, e_2) \leq d_{C_{max}} \end{cases}$$

where:

- $d_\omega(e_1, e_2) = |\omega_1 - \omega_2|$ is the difference in orientation between the two ellipses;
- $d_\alpha(e_1, e_2) = |\alpha - \frac{\omega 1 + \omega_2}{2} + \frac{\pi}{2}|$ is a measure that checks that the ellipses are not shifted, α being the angle between the line that unites the centers of the two ellipses and the horizontal;
- $d_C(e_1, e_2) = |d(c_1, c_2) - (b_1 + b_2)|$, where $d(c_1, c_2)$ stands for the Euclidean distance between the centers of the ellipses.

The alignment interaction is graphically represented in Figure 2 (right).
We assume that all the objects in the image have the same global orientation ω_N. Therefore, the second part of the prior term is given by:

$$U_{al_\omega}(e) = \begin{cases} U^p_{al}(\mathbf{x} \cup e) - U^p_{al}(\mathbf{x}) & \text{if } |\omega_e - \omega_N| \leq d_{\omega_{max}} \\ 0 & \text{otherwise} \end{cases}$$

where $U^p_{al}(\mathbf{x})$ is given by:

$$U^p_{al}(\mathbf{x}) = \gamma_{al} \sum_{1<i<j<n(\mathbf{x})} U_{al}(e_i, e_j).$$

$U_{al}(e_i, e_j)$ is the energy associated to the aligment interaction $\sim_{al}$ and is given by:

$$U_{al}(e_i, e_j) = \begin{cases} \delta\varpi(d_\alpha(u_1, u_2), d_{\alpha_{max}}) & \text{if } u_1 \sim_{alig} u_2 \\ 0 & \text{otherwise} \end{cases}$$

with:

$$\varpi(x, x_{max}) = -\frac{1}{x^2_{max}}[\frac{1 + x^2_{max}}{1 + x^2} - 1], \ for\ x \leq x_{max}$$

being a reward function previously introduced in [6].
This model uses the parameter ω_N for the global direction of the objects to be extracted. This parameter was extracted by trial and error in [1]. We extend the model by automatically computing this parameter.

3 Object orientation using mathematical morphology

The orientation of objects in an image can be identified by ploting the *rose of directions* [8, 9]. The rose of directions consists in representing the polar diagram that indicates the amount of image structures in each direction. Opening and closing operations (opening for bright image structures and closing for dark image structures) are used for directional filtering via mathematical morphology. We apply this method in order to identify the orientation of the docks in the considered harbor. We motivate this approach by the fact that docks are represented as long lines in the images, being thus, easier to identify. We then assume that the orientation of the objects to be extracted (i.e. boats) is perpendicular to the orientation of the docks.

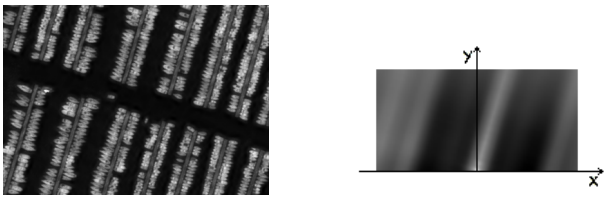

FIG. 3: left: Boats in harbor image ©CNES; right: The corresponding rose of direction by openings

Since the objects we are interested in (i.e. docks) are brighter than the background (i.e. water), opening operations are used. For 2-D gray-scale images, the value of the gray-level rose of directions by opening operations at pixel (i, j) is defined as the volume of the image opened by a discrete line segment of length $2\max\{|i|, j\} + 1$ in pixels, called structuring element (SE), having the orientation defined by $\arctan j/i$. The volume of an image is defined as the sum of its pixel values. By rotating the SE in a discrete manner under all angles in the interval $[0, \pi)$ and by modifying its length, we can identify predominant orientations for bright line structures. The output of the rose of directions is illustrated in Figure 3 (right).
The bright line starting at the origin of the coordinate system in the diagram on the right represents the predominant orientation of bright line structures in the image. Identical values in all directions would indicate that there is no predominant orientation in the image.

4 Results and discussions

Boat extraction results are shown in Figure 4. We highlight errors caused by wrong orientation (i.e. boats having a different orientation than the global orientation considered) in green. The extraction lasted $32min$ and $38sec$ for Figure 4(a), $29min$ and $54sec$ for Figure 4(b) and $55min$ and $21sec$ for Figure 4(c). The computation time for the

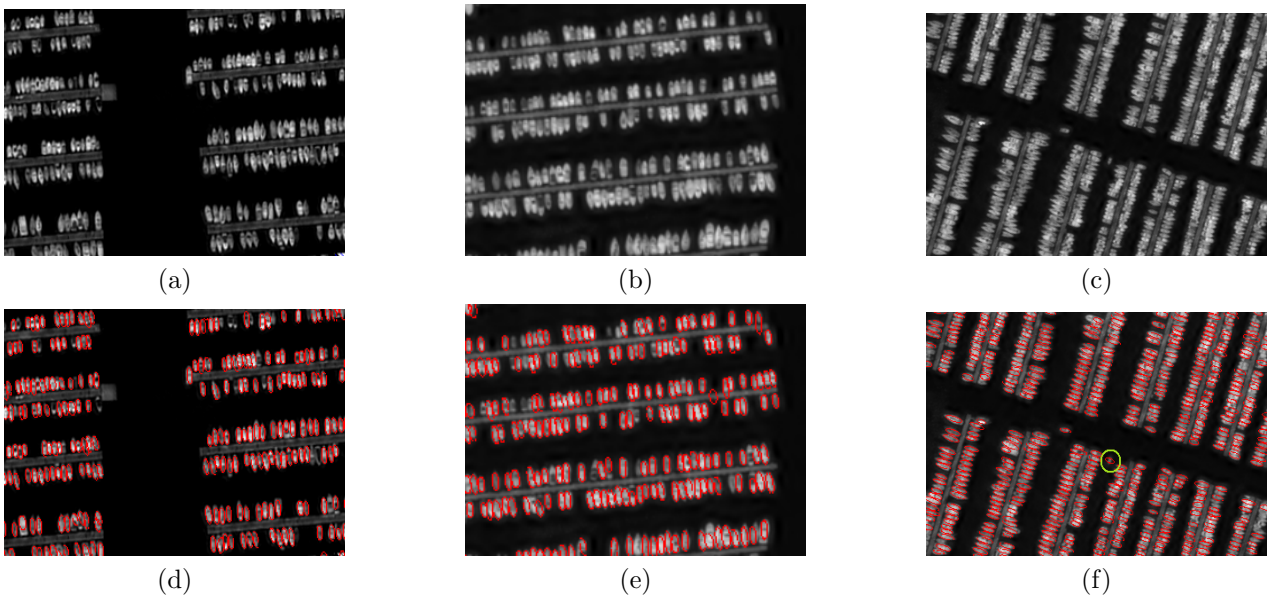

(a) (b) (c)

(d) (e) (f)

FIG. 4: (a) - (c) Images of boats in harbors ©CNES; (d) - (f) Extraction results using the proposed model.

global orientation of the objects is of the order of seconds.

Boat Image	No. of boats extracted	Ground truth	Overall detection error
Figure 4 (a)	233	234	7.2%
Figure 4 (b)	206	204	4.3%
Figure 4 (c)	523	518	1.0%

TAB. 1: Quantitative results and overall detection error

Quantitative results are presented in Table 1. The ground truth was determined by hand by an expert.

5 Conclusions

We have shown that mathematical morphology provides a good alternative for the computation of a key parameter of a MPP model (i.e. global orientation). We have studied a particular type of harbors, in which all boats have the same orientation. The results are very good for this type of harbors. The next open problem to be solved is handling harbors where the boats have different orientations. In this case, imposing a global orientation is not applicable anymore. Therefore, we should propose a new MPP model in a near future in which we take the local orientation of the boats into account to solve this problem.

References

[1] S. Ben Hadj, F. Chatelain, X. Descombes, and J. Zerubia. Parameter estimation for a marked point process within a framework of multidimensional shape extraction from remote sensing images. *Proc. of ISPRS*, XXXVIII, 2010.

[2] F. Chatelain, X. Descombes, and J. Zerubia. Parameter estimation for a marked point process. application to object extraction from remote sensing images. *Proc. of EMMCVPR*, 5681:221–234, 2009.

[3] C. J. Geyer. Likelihood inference for spatial point processes. In *Stochastic geometry, likelihood and computation*. CRC Press, 1999.

[4] C. J. Geyer and J. Møller. Simulation procedures and likelihood inference for spatial point processes. *Scandinavian Journal of Statistics*, 21:359–373, 1994.

[5] P. Green. Reversible jump Markov Chain Monte Carlo computation and Bayesian model determination. *Biometrika*, 82(4):711–732, 1995.

[6] M. Ortner, X. Descombes, and J. Zerubia. A marked point process of rectangles and segments for automatic analysis of Digital Elevation Models. *IEEE Transactions of Pattern Analysis and Machine Intelligence*, 30:105–119, 2008.

[7] G. Perrin, X. Descombes, and J. Zerubia. A marked point process model for tree crown extraction in plantations. *Proc. ICIP*, 1:661–664, 2005.

[8] J. Serra. *Image Analysis and Mathematical Morphology*. Academic Press, 1982.

[9] P. Soille and H. Talbot. Image structure orientation using mathematical morphology. *Proc. of ICPR*, 2:1467–1469, 1998.

[10] D. Stoyan, W. S. Kendall, and J. Mecke. *Stochastic Geometry and its Applications*. John Wiley and Sons, 1987.